Remote Sensing Letters

ISSN: 2150-704X (Print) 2150-7058 (Online) Journal homepage: https://www.tandfonline.com/loi/trsl20

Calibration and validation of the Australian fractional cover product for MODIS collection 6

Juan Pablo Guerschman & Michael J. Hill

To cite this article: Juan Pablo Guerschman & Michael J. Hill (2018) Calibration and validation of the Australian fractional cover product for MODIS collection 6, Remote Sensing Letters, 9:7, 696-705, DOI: 10.1080/2150704X.2018.1465611

To link to this article: https://doi.org/10.1080/2150704X.2018.1465611

Published online: 17 May 2018.

REMOTE SENSING LETTERS
2018, VOL. 9, NO. 7, 696–705
https://doi.org/10.1080/2150704X.2018.1465611

Taylor & Francis
Taylor & Francis Group

Calibration and validation of the Australian fractional cover product for MODIS collection 6

Juan Pablo Guerschman [a] and Michael J. Hill [b,c]

[a]CSIRO Land and Water, Black Mountain, ACT, Australia; [b]Department of Earth System Science and Policy, University of North Dakota, Grand Forks, North Dakota, USA; [c]College of Science and Engineering, Flinders University, South Australia, Australia

ABSTRACT

Fractional cover of photosynthetic vegetation (F_{PV}), non-photosynthetic vegetation (F_{NPV}) and bare soil (F_{BS}) is an important input for assessment of the productivity of global pastures and rangelands. Here we describe the updating of this product using the new Moderate Resolution Imaging Spectroradiometer (MODIS) Nadir BRDF-Adjusted Reflectance (NBAR) Collection 6 reflectance product (C6) and a major expansion of the field calibration database. Fractional cover based on the C6 input exhibited reduced bias and root mean square error compared with the Collection 5 (C5) product. The expanded calibration database with more sites in arid areas provided greater separation between reflectance values of end-members for F_{NPV} and F_{BS}. Specific site variations in F_{NPV} and F_{BS} in arid areas could be traced to small but consistent changes in blue and green band, and occasional changes in short wave infrared reflectance in C6 when compared to C5. The recalibration described here provides an Australian fractional cover product with reduced uncertainty and improves the basis for a prototype global product for use in modelling of rangeland and pasture productivity.

ARTICLE HISTORY
Received 10 November 2017
Accepted 6 April 2018

1. Introduction

A 500 m resolution 8 day fractional cover product based on unmixing reflectances from the Moderate Resolution Imaging Spectroradiometer (MODIS) Nadir Bidirectional Reflectance Distribution Function (BRDF) Adjusted Reflectance Collection 5 (NBAR: MCD43A4.005 hereafter referred to as C5) was developed for Australia over the period from 2009–2015 (Guerschman et al. 2009; Guerschman et al. 2015). The product provides estimates of fractions of photosynthetic vegetation (F_{PV}), non-photosynthetic vegetation (F_{NPV}) and bare soil (F_{BS}) based on linear unmixing of reflectances (Guerschman et al. 2015). The product is a vital component of the Australian Government Ground cover monitoring project (http://www.agriculture.gov.au/ag-farm-food/natural-resources/soils/monitoring/ground-cover-monitoring-for-australia) and is used in a number of active monitoring programs such as DustWatch (dustwatch.edu.au), the State of the Environment reports (soe.environment.gov.au) and the Australian National University's Environment Explorer (wenfo.

CONTACT Juan Pablo Guerschman juan.guerschman@csiro.au CSIRO Land and Water, Black Mountain, ACT, Australia, 2601, Australia

org/ausenv). This product has been extended to provide global fractional cover through the map web portal (map.geo-rapp.org) for the Group on Earth Observations GLobal Agricultural Monitoring Rangeland and Pasture Productivity (GEOGLAM RAPP) (Youngentob et al. 2014; Guerschman et al. 2015). Along with standing biomass and growth rate, fractional cover represents one of three vital inputs for assessment of sustainable global rangeland productivity.

A new MODIS MCD43A4.006 (C6) daily product has now been released based on 16 day rolling retrievals and weighted to estimate the BRDF/Albedo at the first day of the second 8-day period (Schaaf and Wang 2015). Given the national and international importance of fractional cover product, it is essential to apply the fractional cover algorithm with the MODIS C6 NBAR and provide an updated product to both Australian and international users.

The product was developed using an extensive ground calibration dataset (designated hereafter as D5; Muir et al. 2011; Scarth et al. 2015; http://www.auscover.org.au/purl/slats-star-transects-all-sites). An initial processing of C6 based on the original calibration and ground data produced a problematic overall shift towards lower F_{NPV} and higher F_{BS} relative to the C5 product. Fortunately, the ground dataset had recently been substantially enhanced to provide more complete geographical coverage and more than twice as many sites (designated hereafter as D6). Therefore, this paper presents the results of a re-calibration and validation based on C6 and D6, identifies issues and improvements arising from the implementation of the new data sets, and points to future more comprehensive scientific studies and applications arising.

2. Materials and methods

2.1. *Data*

The MODIS MCD43A4.006 NBAR (C6) is a daily 16-day product at Stage 3 validation. The dating system has been adjusted to tag each image to the 9th day of the 16 day retrieval period (C5 uses the first day). This C6 product is produced using a number of improved methods which could result in small changes to the BRDF adjusted reflectances: weighting of observations to the first day of the second 8 day period; an improved pixel-based back-up database; use of more observations at high latitudes; and input from the L2G lite surface reflectance (MOD09GA) (Schaaf and Wang 2015). The C5 NBAR was discontinued after March 2017, thus both the Australian and and prototype global fractional cover products have to be transitioned to C6.

The D5 used by Guerschman et al. (2015) has been substantially expanded from 1171 to 3022 sites (D6; Figure 1). A large number of sites have been added across the Northern Territory providing much stronger data for systems with higher F_{BS} and F_{NPV}, and the distribution of sites throughout Queensland is improved. A small number of sites (shown in yellow; Figure 1) were removed due to uncertainties about data quality. The D6 database conforms to the same sampling procedures outlined by Muir et al. (2011) and Guerschman et al. (2015). The field measurements include cover fractions in the understorey and, if present, the mid-storey (shrubs) and overstorey (trees). We incorporated the three strata into an exposed planar fraction cover (what we refer to as F_{PV}, F_{NPV} and F_{BS} in this paper) to compare these measurements with satellite estimates following

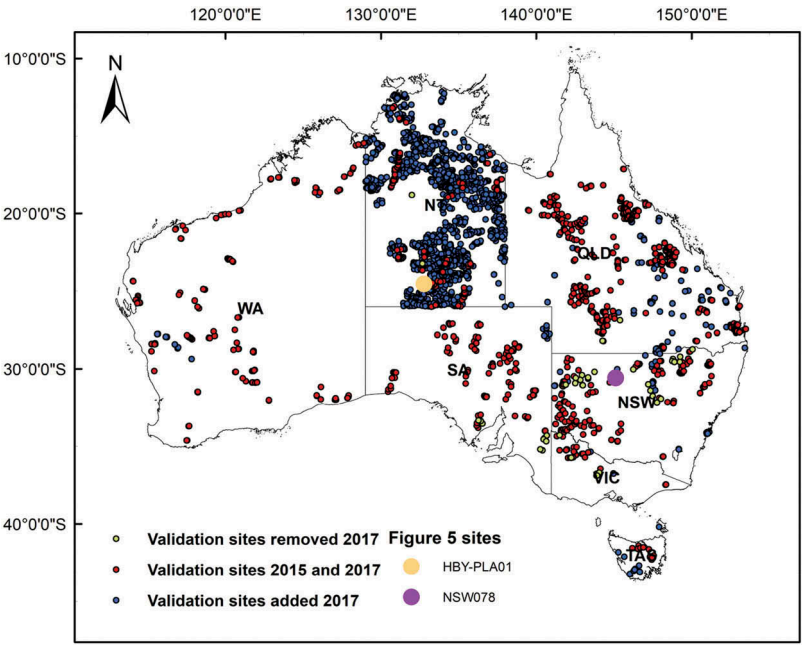

Figure 1. Map of Australia showing the additional calibration sites added (in blue), the original sites shared with the new data set (in red) and a few shared sites removed from the new data due to quality limitations (in yellow). The location of sites selected for closer examination in Figure 4 is also shown. State abbreviations: NSW – New South Wales; VIC – Victoria; QLD – Queensland; SA – South Australia; WA – Western Australia; NT – Northern Territory; TAS – Tasmania; and ACT – Australian Capital Territory.

Guerschman et al. (2015; see Section 2.1 therein). The approach assumes that the distribution of each strata is not affected by the clumpiness of the strata above.

The new fractional cover product discussed here is derived by the same method as outlined in Guerschman et al. (2015; please see this article for the full method) in which linear unmixing (Plaza et al. 2012) is applied using all seven reflectance bands with log transforms and band interaction terms being incorporated to account for non-linearities (Armston et al. 2009). In particular, this model inverts the field datasets and derives end-members by regressing the reflectance values against the field data (Dobigeon et al. 2014; Puyou-Lascassies et al. 1994). The resulting multiple regression coefficients are inverted and non-linear influences are captured by including log transforms for each band, the product of all bands, the product of the log transforms of each band, and the normalised ratio for all band combinations (Armston et al. 2009). Endmembers are then derived by minimizing the root mean square errors from a hundred-fold cross validation against the field sites with 50% of points used for determining end-members and the other 50% used for unmixing (Guerschman et al. 2015). This approach demonstrated improved root mean square errors (RMSE) for F_{NPV} and F_{BS} over previous approaches to derivation of fractional cover (Guerschman et al. 2009; Guerschman et al. 2015). The calibration method is applied either with D5 and C5 (Cal5) or D6 and C6 (Cal6). The resulting endmembers for unmixing (Cal5 or Cal6) are tested with D5 and D6 and C5 and C6.

2.2. *Analysis*

The analysis was carried out for pixels corresponding to the field data locations. In the first instance. The following combinations of data, calibration and MODIS collection for deriving FC were examined: C5D5Cal5; C5D6Cal5; C6D6Cal5; C5D6Cal6; and C6D6Cal6. Field measurements of fractional cover, image-based fractional cover and reflectance values were extracted and compared. A subset of 100 sites was randomly selected from the sites common to C5 and C6 time periods. MODIS C5 and C6 reflectance and derived fractional cover profiles were examined for a six year subset of the time series (2001–2006) to explore differences due to the new site database and MODIS product.

3. Results and discussion

Comparison C5D5Cal5 and C6D5Cal5 showed a negative deviation from the 1:1 line for F_{NPV} and a positive deviation for F_{BS} (Figure 2(a); Table 1). This indicated that the old Cal5 could not be used with the MODIS C6 without introducing bias. When C5D6Cal5 and C5D6Cal6 were compared, the correspondence was good but a small shift in the F_{BS} was evident (Figure 2(b). This suggested that the D6 was providing better coverage of the fractional cover domain than the D5, but that some small systematic effects due to the C6 were still present. When the original C5D5Cal5 product was compared with the C6D6Cal6 fractional cover product alignment was good (Figure 2(c)), but both the root mean square error (RMSE) and bias were reduced for the C6D6Cal6 version (Table 1). The comparison of observed and estimated values for F_{PV}, F_{NPV} and F_{BS} for C6D6Cal6 (Figure 2(d)) showed an improvement in the correlation coefficient (r), RMSE and bias for NPV and BS when compared with the C5D5Cal5 product (Table 1; Guerschman et al. 2015). The additional field sites were primarily located in arid and semi-arid areas of the Northern Territory and inland Queensland providing greatly enhanced sampling of F_{BS} and F_{NPV} than was available the C5D5Cal5 product. As a result uncertainty in estimation of F_{BS} and F_{NPV} is reduced.

Comparison of the endmembers derived from the C6D6Cal6 and C5D5Cal5 processes showed small but important changes in reflectance values for all three cover fractions (Figure 3): small reductions in R_{469} and R_{555} for PV; small increases in R_{858} and R_{1640} for NPV; and small increases in R_{645} and R_{858}, and slightly larger increases in R_{1640} and R_{2135} for BS (where R_x is the reflectance in the x wavelength measured in nm). This resulted in a larger separation between the F_{NPV} and F_{BS} end-members, especially in the short wave infrared where much of the spectral sensitivity to soil reflectance and cellulose absorption is located (Guerschman et al. 2009).

A comparison between the long term mean (2001–2016) fractional cover for C5D5Cal5 and C6D6Cal6 is presented in Figure 4. Significant differences between the two products in the F_{NPV} can be observed throughout much of the arid inland and western half of the Continent. C6D6Cal6 produced estimates ~10–15% higher than C5D5Cal5 across much of the arid inland. This pattern was mirrored by decreases in F_{BS} across the same area although the magnitude of these changes was lower. Small differences in F_{PV} are observed at low cover fractions in the southeast.

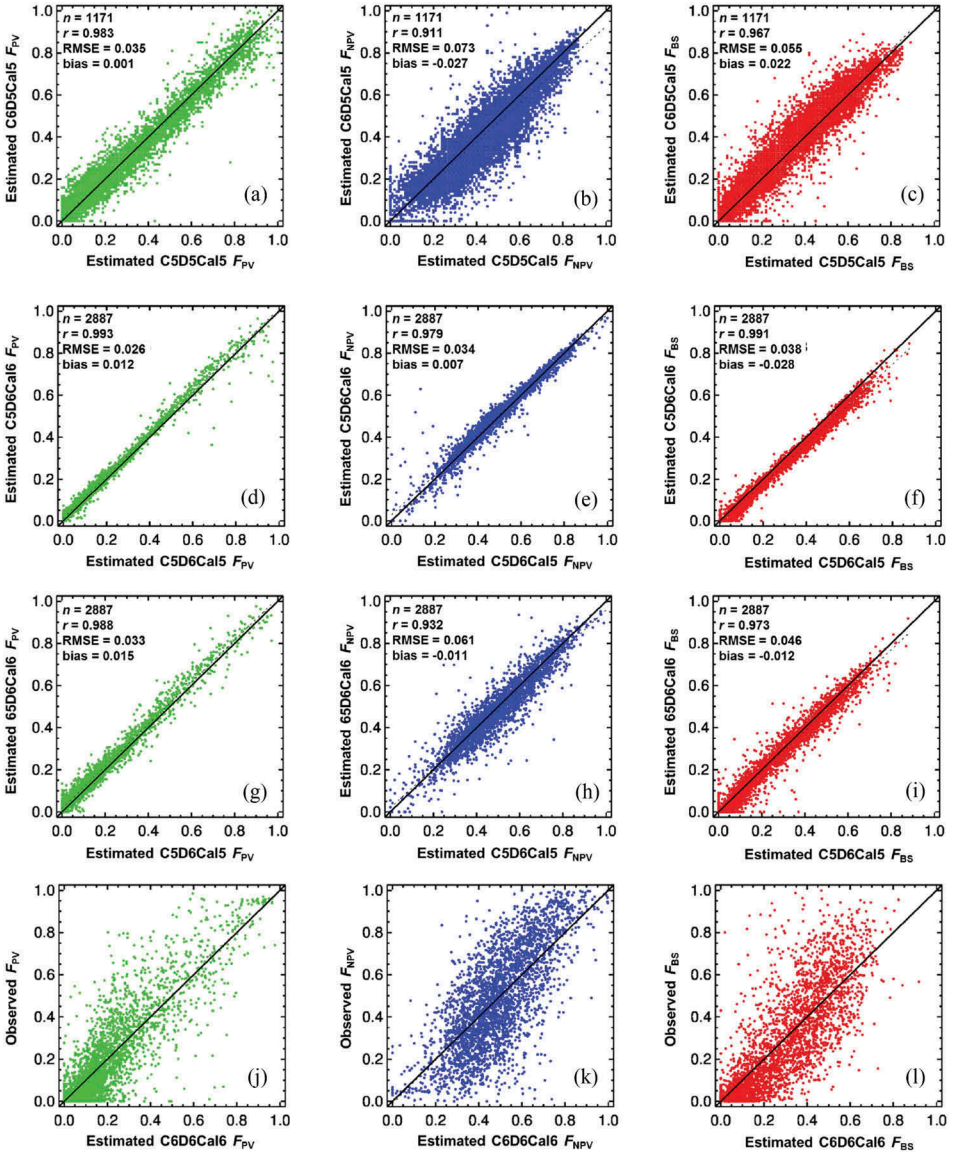

Figure 2. (a)-(c) Comparison of F_{PV}, F_{NPV} and F_{BS} between C5D5Cal5 and C6D5Cal5; (d)-(f) Comparison of F_{PV}, F_{NPV} and F_{BS} between C5D6Cal5 and C5D6Cal6; (g)-(i) Comparison of F_{PV}, F_{NPV} and F_{BS} between C5D6Cal5 with C6D6Cal6 showing good alignment along the 1:1 line; and (j)-(l) Validation of F_{PV}, F_{NPV} and F_{BS} for C6D6Cal6 with the enhanced site database. The statistics for (j)-(l) appear in Table 1.

Profiles for two sites located in more arid regions (Figure 5) illustrate the differences throughout the time series attributable to some systematic variation in C6 compared to C5. Sites where F_{NPV} and F_{BS} varied significantly between the C5D5Cal5and C6D6Cal6 products were associated primarily with consistent differences in blue and green band reflectance between C5 and C6 (Figure 4(a, b)). These differences resulted in an increase in F_{NPV} and decrease in F_{BS} for C6D6Cal6 versus C5D5Cal5 throughout much of the time

Table 1. Comparison of calibration statistics for all combinations of MODIS collections and calibration field sites. Comparisons for C6 are based on field measurements from D6. Comparisons for MODIS C5 are based both the original sites (*C5) and on the new sites that existed prior to the end of the product in March 2017 (#C5).

MODIS collection	Calibration	number of observations	Product	R^2	RMSE	Bias
*C5	D5Cal5	1171	F_{PV}	0.832	0.129	−0.006
		1171	F_{NPV}	0.643	0.181	0.003
		1171	F_{BS}	0.736	0.166	−0.002
#C5	D6Cal5	2887	F_{PV}	0.861	0.116	0.016
		2887	F_{NPV}	0.708	0.165	−0.015
		2887	F_{BS}	0.791	0.150	−0.016
#C5	D6Cal6	2887	F_{PV}	0.854	0.117	0.004
		2887	F_{NPV}	0.697	0.168	−0.022
		2887	F_{BS}	0.785	0.151	0.012
C6	D6Cal5	3022	F_{PV}	0.860	0.114	0.010
		3022	F_{NPV}	0.710	0.164	0.005
		3022	F_{BS}	0.784	0.153	−0.030
C6	D6Cal6	3022	F_{PV}	0.861	0.113	−0.000
		3022	F_{NPV}	0.722	0.161	−0.001
		3022	F_{BS}	0.793	0.147	−0.006

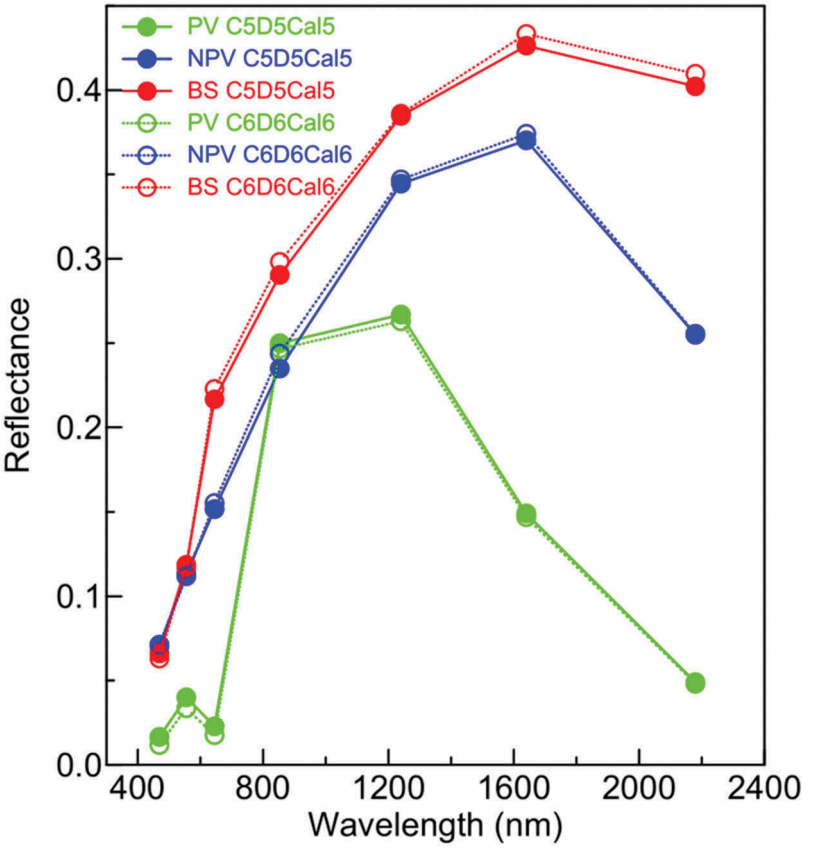

Figure 3. Comparison of end-members for PV, NPV and BS between the C5D5Cal5 and C6D6Cal6 processes showing changes in relativities between blue and green reflectance and increased separation between NIR and SWIR reflectances for C6D6Cal6 versus C5D5Cal5.

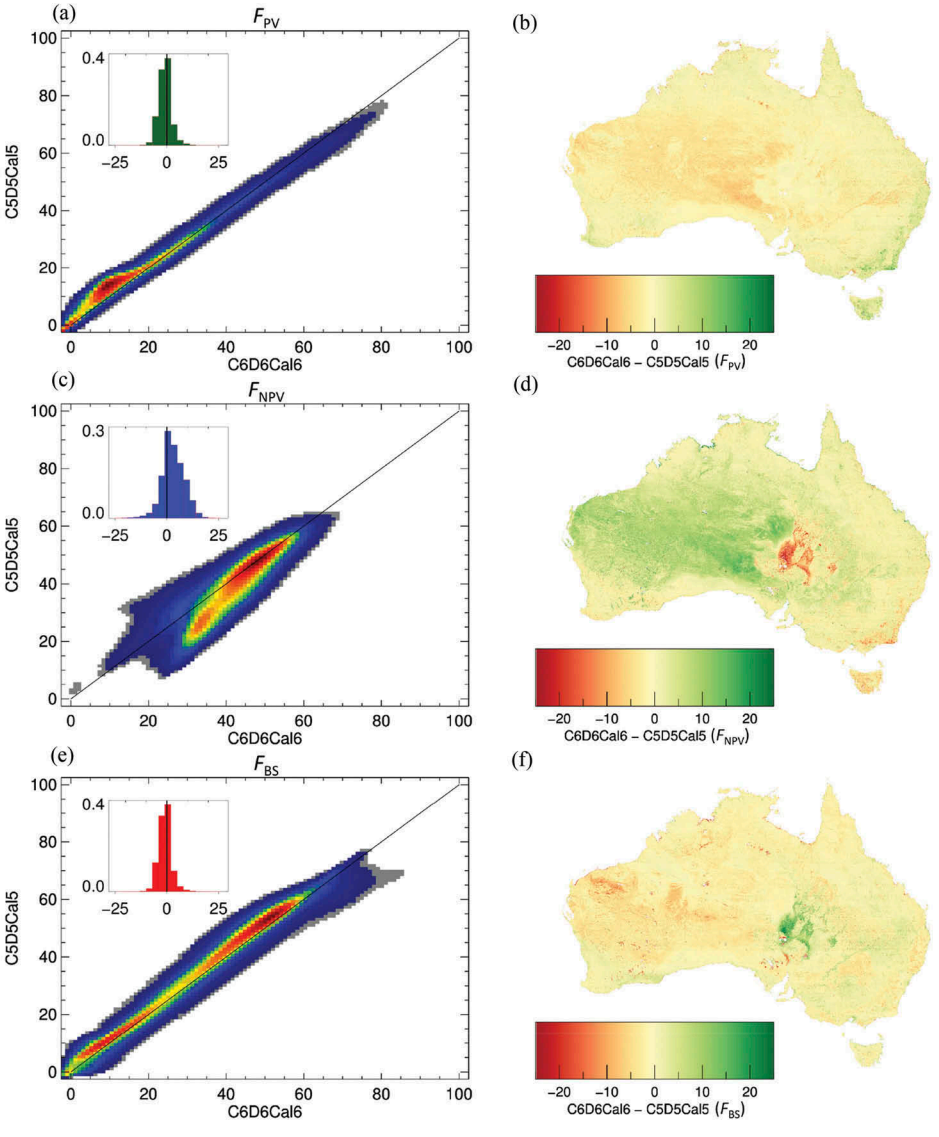

Figure 4. Comparison of the differences in the long term (2001–2015) mean values of F_{PV} (a), (b), F_{NPV} (c), (d), and F_{BS} (e), (f), between C5D5Cal5 and C6D6Cal6. The scatterplots show the density of pixels ((a), (c), (e)). The inset histograms show the frequency of the differences between C6D6Cal6 and C5D5Cal5. The maps ((b), (d), (f)) show the spatial distribution of differences between versions.

series. In most higher rainfall northern and southern region sites exhibited excellent correspondence between C5D5Cal5 and C6D6Cal6 for F_{PV}, F_{NPV} and F_{BS} (individual data not given; see Figure 4). Previous studies have emphasised the dependence on reflectance above 2000 nm for discrimination between F_{NPV} and F_{BS} (Asner and Lobell 2000) but it is evident here that blue band reflectance over arid land bright targets is also important.

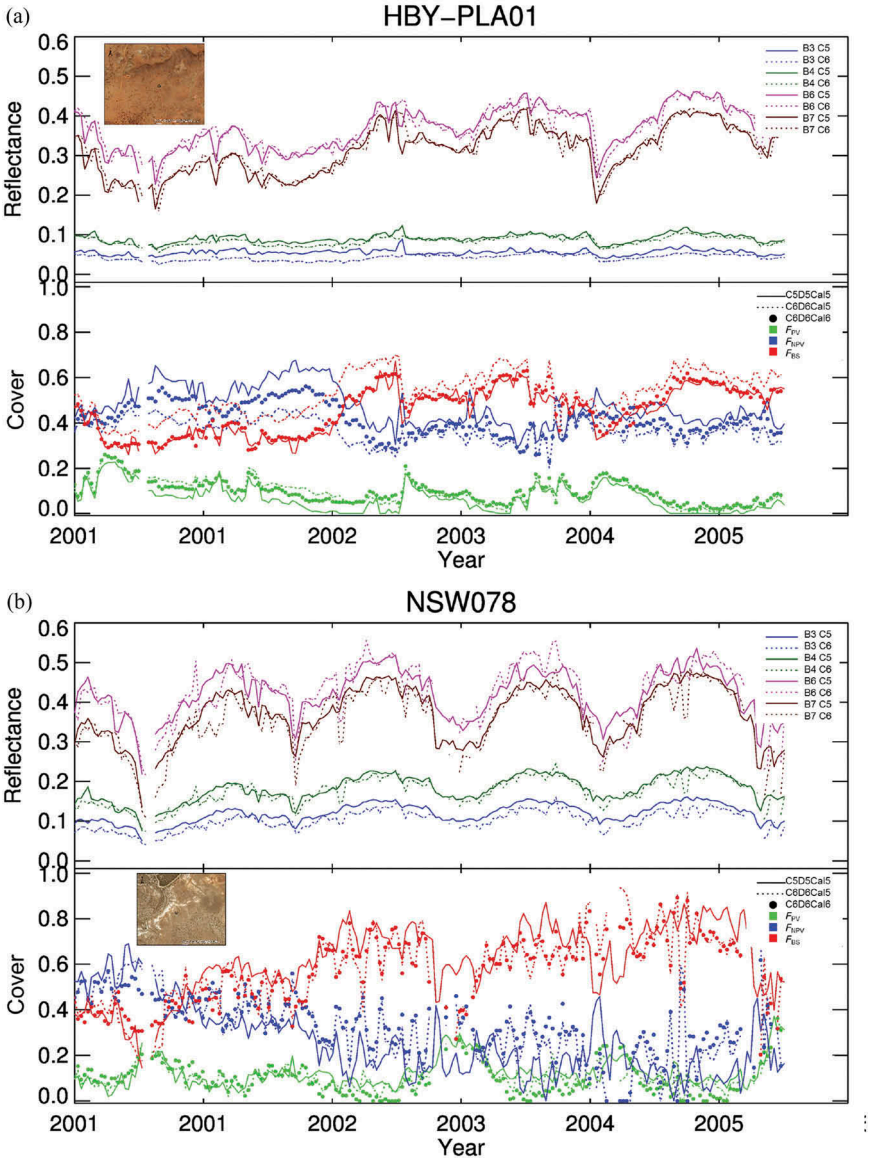

Figure 5. Time series for 2001 – 2006 for MODIS collection 5 and collection 6 reflectances and corresponding fractional cover at selected calibration sites in the arid areas which exhibit deviations in reflectance and F_{NPV} and F_{BS} between collections: (a) HBY-PLA01 – note the Blue band 3; (b) NSW078 – note the Blue band 3 and SWIR band 7 (Locations shown in Figure 1. Images obtained from ArcGIS are © 2017 DigitalGlobe).

4. Conclusions

The new C6D6Cal6 fractional cover product maintains consistency with the previous C5D5Cal5 version and exhibits improvements in RMSE and coefficient of determination (R^2) and reductions in bias. However consistent differences in R_{469} and intermittent differences in reflectance in the R_{1640} and R_{2135} between C5 and C6 result in slightly higher F_{NPV} and lower F_{BS} in arid locations. The MODIS Adaptive Processing System is generating an

improved Collection 6.1 (C6.1) for MODIS Level 1 (L1) and higher level atmospheric products due to the need to change calibration to account for: a) a Response-Versus-Scan angle approach that affects reflectance bands due to Top-of-Atmosphere reflectance drift in bands 1–4 of MODIS Aqua; and b) a correction to the Tera MODIS forward Look-Up Table for 2012–2017 (MODAPS 2017). The Australian fractional cover product will be reprocessed using C6.1 inputs when these become available. However, the improved RMSE, R^2 and reduced bias for F_{NPV} and F_{BS} obtained with the D6C6Cal6 combination emphasises the importance of a comprehensive field database for calibration of fractional cover retrievals. A recent application of a similar approach in China only achieved an RMSE of 0.257 and an R^2 of 0.375 for F_{NPV} with much more limited ground data for calibration and validation (Li et al. 2017). A new global fractional cover dataset based on C6-6.1 is now available at the GEOGLAM RAPP MAP website (http://www.geo-rapp.org/geoglam-rapp-map-online/) and further expanded studies will be forthcoming from this dataset.

Acknowledgments

We thank Rebecca Trevithick and Jasmine Muir for access to the updated field database for fractional cover calibration and validation. This project is supported by Michele Barson, through funding from the Australian Government's National Landcare Program. GEOGLAM RAPP is an initiative of CSIRO, GEO and GEOGLAM.

Funding

This work was supported by the the Australian Government's National Landcare Program.

ORCID

Juan Pablo Guerschman http://orcid.org/0000-0001-7464-6304
Michael J. Hill http://orcid.org/0000-0003-4570-7467

References

Armston, J. D., R. J. Denham, T. J. Danaher, P. F. Scarth, and T. N. Moffiet. 2009. "Prediction and Validation of Foliage Projective Cover from Landsat-5 TM and Landsat-7 ETM+ Imagery." *Journal of Applied Remote Sensing* 3: 33528–33540. doi:10.1117/1.3216031.

Asner, G. P., and D. B. Lobell. 2000. "A Biogeophysical Approach for Automated SWIR Unmixing of Soils and Vegetation." *Remote Sensing of Environment* 74: 99–112. doi:10.1016/S0034-4257(00)00126-7.

Dobigeon, N., J.-Y. Tourneret, C. Richard, J. C. M. Bermudez, S. McLaughlin, and A. O. Hero. 2014. "Nonlinear Unmixing of Hyperspectral Images: Models and Algorithms." *Signal Processing Magazine, IEEE* 31 (1): 82–94. doi:10.1109/MSP.2013.2279274.

Guerschman, J. P., A. A. Held, R. J. Donohue, L. J. Renzullo, N. Sims, F. Kerblat, and M. Grundy. 2015. "The GEOGLAM Rangelands and Pasture Productivity Activity: Recent Progress and Future Directions." Presented at 2015 Fall Meeting, AGU, San Francisco, CA, December 14–18. http://adsabs.harvard.edu/abs/2015AGUFM.B43A0531G.

Guerschman, J. P., M. J. Hill, L. J. Renzullo, D. J. Barrett, A. S. Marks, and E. J. Botha. 2009. "Estimating Fractional Cover of Photosynthetic Vegetation, Non-Photosynthetic Vegetation and Bare Soil in the Australian Tropical Savanna Region Upscaling the EO-1 Hyperion and MODIS Sensors." *Remote Sensing of Environment* 113: 928–945. doi:10.1016/j.rse.2009.01.006.

Guerschman, J. P., P. F. Scarth, T. R. McVicar, L. J. Renzullo, T. J. Malthus, J. B. Stewart, J. E. Rickards, and R. Trevithick. 2015. "Assessing The Effects Of Site Heterogeneity and Soil Properties When Unmixing Photosynthetic Vegetation, Non-photosynthetic Vegetation and Bare Soil Fractions from Landsat and Modis Data." *Remote Sensing Of Environment* 161: 12–26. doi: 10.1016/j.rse.2015.01.021.

Li, X., Z. Li, C. Ji, H. Wang, B. Sun, B. Wu, and Z. Gao. 2017. "A 2001–2015 "Archive of Fractional Cover of Photosynthetic and Non-Photosynthetic Vegetation for Beijing and Tianjin Sandstorm Source Region." *Data* 2: 27. doi:10.3390/data2030027.

MODAPS. 2017. "Level-1B (L1B) Calibration Collection 6.0 And Collection 6.1 Changes. Terra and Aqua MODIS." C061_L1B_Combined_v9.pdf. https://modis-atmos.gsfc.nasa.gov/documentation/collection-61.

Muir, J., M. Schmidt, D. Tindall, R. Trevithick, P. Scarth, and J. B. Stewart. 2011. *Field Measurement of Fractional Ground Cover: A Technical Handbook Supporting Ground Cover Monitoring for Australia*. Canberra: Queensland Department of Environment and Resource Management for the Australian Bureau of Agricultural and Resource Economics and Sciences.

Plaza, J., E. T. Hendrix, I. García, G. Martín, and A. Plaza. 2012. "On Endmember Identification in Hyperspectral Images without Pure Pixels: A Comparison of Algorithms." *Journal of Mathematical Imaging and Vision* 42: 163–175. doi:10.1007/s10851-011-0276-0.

Puyou-Lascassies, P., G. Flouzat, M. Gay, and C. Vignolles. 1994. "Validation of the Use of Multiple Linear Regression as a Tool for Unmixing Coarse Spatial Resolution Images." *Remote Sensing of Environment* 49: 155–166. doi:10.1016/0034-4257(94)90052-3.

Scarth, P., J. P. Guerschman, K. Clarke, and S. Phinn. 2015. "Validation of Australian Fractional Cover Products from MODIS and Landsat Data." In *AusCover Good Practice Guidelines: A Technical Handbook Supporting Calibration and Validation Activities of Remotely Sensed Data Product*, edited by A. Held, S. Phinn, M. Soto-Berelov, and S. Jones, 123–138. Version 1.2. St Lucia: TERN AusCover. ISBN 978-0-646-94137-0.

Schaaf, C. B., and Z. Wang. 2015. "MCD43A4 MODIS/Terra+Aqua BRDF/Albedo Nadir BRDF Adjusted RefDaily L3 Global - 500m V006." *NASA EOSDIS Land Processes DAAC*. doi:10.5067/modis/mcd43a4.006.

Youngentob, K. N., A. A. Held, M. Grundy, and R. J. Donohue. 2014. "Establishment of the GEOGLAM Rangelands Activity and Progress." Abstract B43G-01 presented at 2014 Fall Meeting, AGU, San Francisco, CA, December 15–19. http://abstractsearch.agu.org/meetings/2014/FM/B43G-01.html.